Communication

Low-Cost Compact Circularly Polarized Dual-Layer PIFA for Active RFID Reader

Libin Sun, Yue Li, Zhijun Zhang, and Magdy F. Iskander

***Abstract*— This communication presents a novel single-fed compact circularly polarized (CP) dual-layer planar inverted-F antenna (PIFA). The proposed antenna is composed of two stacked orthogonal-orientated PIFAs which can be fabricated by elaborately folding one piece of metal plate. The two PIFAs can be excited synchronously with equally allocated power by a single probe, thus a pair of orthogonal polarizations is created. Moreover, the resonant lengths of the upper and lower PIFAs are slightly different from each other to acquire 90° phase shift between the two orthogonal polarizations. Consequently, a right-hand CP radiation is achieved, and the boresight realized gain is 3.8 dBic at the center frequency. The proposed dual-layer PIFA with two quarter-wavelength resonators provides a novel solution for the compactness of CP antennas. To validate the performance of the antenna, a prototype was fabricated and measured. The measured −10 dB impedance bandwidth and 3 dB axial ratio bandwidth are 7.4% and 1.1%, respectively, with a compact antenna volume of $0.26 \times 0.22 \times 0.05\ \lambda_0^3$. The proposed antenna is a good candidate for the 433 MHz CP active radio-frequency identification reader, and it has the merits of compact size, lightweight, high efficiency, and low cost.**

***Index Terms*— Circularly polarized (CP), dual layer, planar inverted-F antenna (PIFA), radio-frequency identification (RFID).**

I. Introduction

Circularly polarized (CP) antennas have lots of merits compared with linearly polarized antennas, such as combating the multipath interferences, reducing the Faraday rotation effect and insensitive to the orientations of transmitting and receiving antennas [1], [2]. Therefore, CP antennas are widely applied in a large number of wireless communication systems, such as the radio-frequency identification (RFID) systems to avoid the polarization mismatching [3]–[9]. The active RFID systems operating at Industrial, Scientific, and Medical (ISM) 433 MHz have been widely applied in the medical communication, industrial management, and vehicle identification, and it has the merits of long communication distance and desirable penetrability due to the low frequency [10]. According to the ISO/IEC 18000-7 standard [11], the required bandwidth for the 433 MHz active RFID systems is 433.67–434.17 MHz (500 kHz).

Due to the large wavelength at 433 MHz (about 0.7 m), it is urgent to reduce the physical size of a CP antenna and achieve a desirable broadside gain and axial ratio (AR) bandwidth. Utilizing the dielectric substrate with high permittivity can reduce the size of the antennas effectively [3]. However, the bandwidth of the antenna is narrow, and the dielectric substrate is thick, heavy, and expensive when working at 433 MHz. Thus, air media is preferable for the merits of low cost, lightweight, low Q-factor, and high efficiency [4]–[8]. Some compact CP dipole pairs with parasitic elements are presented in [4]–[6], but it is not suitable for the environment assembled on a metal ground. A meander line disk loaded monopole is reported in [7] with a very compact volume, but the conical radiation pattern is not suitable for this application. Two modified inverted-L antenna elements with double-folded arms are investigated in [8] with a compact size but the profile is as high as 0.14 λ_0.

There are many kinds of literature drawing attention on the compact CP microstrip antennas with the single-fed technique [12]–[23]. Various shaped slots are cut on the patches to lengthen the electrical length of the microstrip antennas and make perturbations to excite two degenerate orthogonal modes with 90° phase shift. About 20%–50% size reductions have been realized compared with the conventional single-fed truncated patch antenna [24]. The techniques proposed in [12]–[23] are all based on modifying the patch antennas with half-wavelength resonance. If the planar inverted-F antennas (PIFAs) with quarter-wavelength resonance are employed to achieve the CP radiation, the size of antennas can be reduced by at least 75% compared with the conventional truncated patch antenna. However, unlike the microstrip antennas [25], a single PIFA does not have two degenerate orthogonal modes due to the asymmetric boundary, therefore, rare literature have presented the CP element by a single PIFA structure.

In this communication, a novel dual-layer PIFA is presented to achieve a compact single-fed CP antenna. Two PIFAs with different orientations are stacked together to create two quarter-wavelength orthogonal modes, and the size difference of the two PIFAs provides the 90° phase shift, thus a CP radiation is achieved. Moreover, the proposed dual-layer stacked structure can be fabricated by folding one piece of metal plate, which is a concise and low cost solution in the engineering region. The proposed antenna has the merits of compact, low cost, lightweight, high efficiency, and ease of manufacture, which is a good candidate for the 433 MHz active RFID readers.

II. Antenna Design

A. Antenna Configuration

Fig. 1 shows the evolution process and three projected views of the proposed CP antenna. Fig. 1(a) illustrates a piece of irregular brass plate, and it can be divided into four surfaces (I, II, III, and IV) by the dashed line. Two holes are drilled in the brass plate to let the feed probe pass. If we fold the brass plate along the dashed line, the antenna's main body is achieved as shown in Fig. 1(b), and the corresponding four surfaces are also illustrated. Then, after adding a metal ground plane and feed probe, the proposed dual-layer PIFA is

Manuscript received March 20, 2018; revised September 27, 2018; accepted October 25, 2018. Date of publication November 9, 2018; date of current version January 16, 2019. This work was supported in part by the National Natural Science Foundation of China under Grant 61525104 and Grant 61771280 and in part by Beijing Natural Science Foundation under Grant 4182029. *(Corresponding author: Zhijun Zhang.)*

L. Sun, Y. Li, and Z. Zhang are with the Beijing National Research Center for Information Science and Technology, Tsinghua University, Beijing 100084, China (e-mail: zjzh@tsinghua.edu.cn).

M. F. Iskander is with the Hawaii Center for Advanced Communications, University of Hawaii at Manoa, Honolulu, HI 96822 USA (e-mail: magdy.iskander@gmail.com).

Color versions of one or more of the figures in this communication are available online at http://ieeexplore.ieee.org.

Digital Object Identifier 10.1109/TAP.2018.2880093

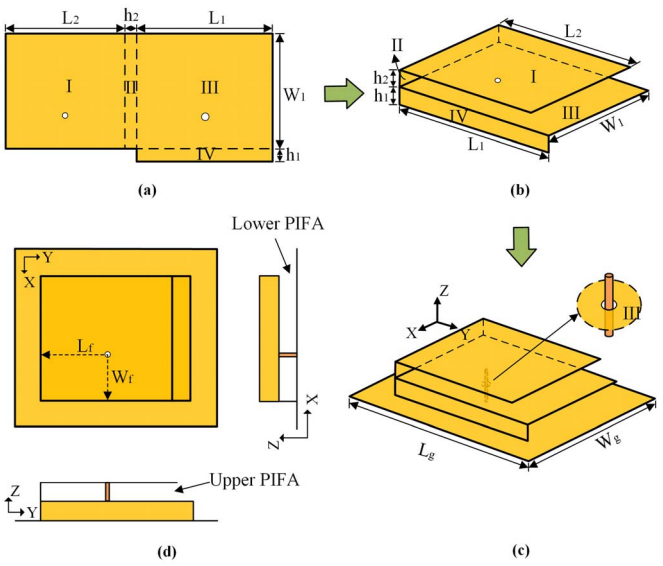

Fig. 1. Evolution process of the proposed antenna. (a) Raw material: a piece of brass plate. (b) Main body of the proposed antenna folded by the brass plate. (c) Final proposed CP dual-layer PIFA. (d) Three projected views of the proposed antenna.

TABLE I
DETAILED DIMENSIONS (UNIT: mm)

Parameter	L_1	L_2	W_1	h_1	h_2
Value	185	162	155	17.5	17.5
Parameter	L_f	W_f	Lg	Wg	
Value	82.5	56.5	250	220	

accomplished as shown in Fig. 1(c). To guarantee the stiffness of the antenna, the structure is sustained by the foam, which is not shown in Fig. 1 for brevity. The feed probe in the surface III is enlarged in Fig. 1(c), as can be seen, the probe passes through the surface III without touching it and the energy will be coupled to the lower PIFA. The end of the probe is soldered with surface I, thus the upper PIFA can be excited directly by the probe. Consequently, the feed probe can excite two PIFAs simultaneously and a good impedance match can be achieved for both PIFAs by finely tuning the feed position. The three projected views of the proposed antenna are plotted in Fig. 1(d). It can be clearly seen that the radiation aperture of the upper PIFA is along the y-direction while that of the lower PIFA is along the x-direction. Therefore, a pair of quarter-wavelength orthogonal modes is achieved by the proposed dual-layer PIFA structure. The resonant frequencies of the lower and upper PIFAs are determined by the resonant edges of PIFAs, i.e., W_1 and L_2, respectively. By finely adjusting two PIFAs' resonant length, 90° phase shift can be obtained in the center frequency. The dimensions of the proposed antenna are optimized by HFSS version 15.0 and the detailed dimensions of the proposed antenna are listed in Table I.

B. Operating Mechanism

In order to illustrate the working mechanism of the proposed dual-layer PIFA, the vector electric field distributions at 433 MHz with different phases are reported in Fig. 2. When $t = 0$, as shown in Fig. 2(a), the upper PIFA is excited with the electric field directing at the $-z$-axis and varying along the y-axis, while the lower PIFA

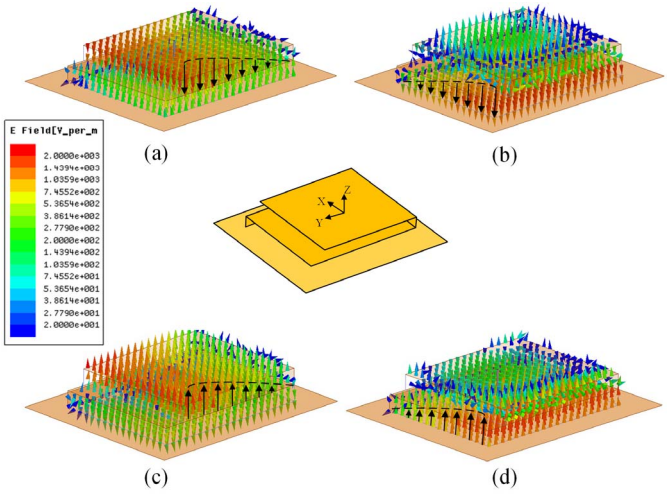

Fig. 2. Vector electric field distributions of the proposed dual-layer PIFA with different phases at 433 MHz. (a) t = 0. (b) t = T/4. (c) t = T/2. (d) t = 3T/4.

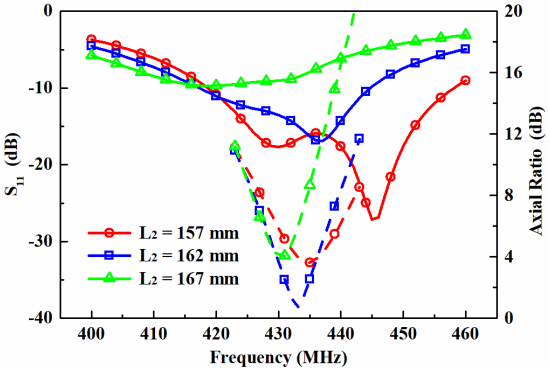

Fig. 3. Simulated S_{11} and AR against frequency for different L_2, the solid line represents the S_{11} and the dashed line represents the AR.

does not work. Therefore, a y-polarization radiation is achieved on the boresight of the antenna. When $t = T/4$, as shown in Fig. 2(b), the lower PIFA is excited with the electric field directing at the $-z$-axis and varying along the x-axis, while the upper PIFA does not work. Therefore, a x-polarization radiation is achieved on the boresight of the antenna. Moreover, 90° phase shift between the two orthogonal modes can be acquired by the different resonant lengths of the upper and lower PIFAs. Consequently, a broadside CP radiation is acquired with the electric field rotating periodically along the circular direction.

C. Antenna Tuning and Parameters Analyzing

As we all know, the resonant frequency of the dominant mode is dependent on the length of the resonant edge and independent of the nonresonant edge. The height of PIFA is also an important parameter to impact the bandwidth and resonant frequency [25]. For the proposed dual-layer PIFA, L_2 and W_1 are the resonant lengths of the upper and lower PIFAs, respectively. The curves of S_{11} and AR with L_2 varied are plotted in Fig. 3. Dual-resonance characteristic can be observed due to the different resonant frequencies of the upper and lower PIFAs. The resonant frequency of the upper PIFA (high frequency) is shifted to lower frequency when increasing L_2, while the resonant frequency of the lower PIFA (low frequency) is almost kept unchanged. With the frequency shift of the upper PIFA, the phase difference between the two PIFAs will deviate from 90°, thus the AR

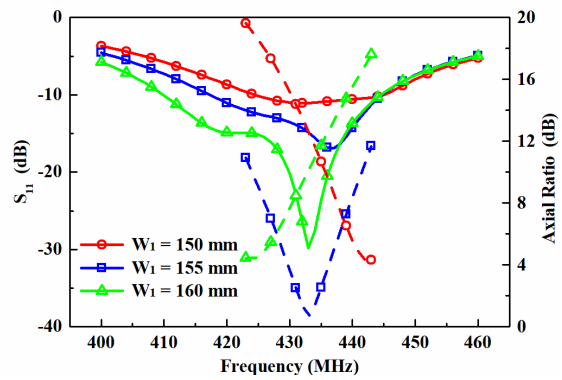

Fig. 4. Simulated S_{11} and AR against frequency for different W_1, the solid line represents the S_{11} and the dashed line represents the AR.

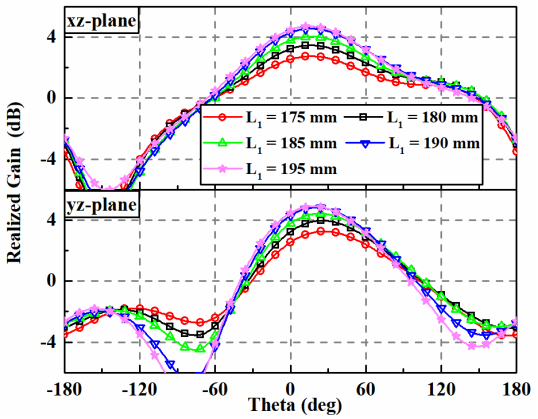

Fig. 5. Simulated radiation patterns in the *xz* and *yz* planes for different L_1.

deteriorates with L_2 varied as shown in Fig. 3. Besides, W_1 is the resonant length of the lower PIFA and also is the nonresonant length of the upper PIFA, the impact of it is analyzed in Fig. 4. Similarly, the resonant frequency of lower PIFA (low frequency) is shifted to lower frequency when increasing W_1, and the deterioration of AR is severer than that of L_2. As for L_1, which is the nonresonant length of the lower PIFA, has little impact on the resonant frequency and AR. However, the surface III plays the role of the upper PIFA's ground plane, thus L_1 has a significant impact on the radiation pattern of the proposed antenna. Fig. 5 shows the radiation patterns in the *xz* and *yz* planes with L_1 varied, the maximum realized gain increases from 3.2 to 4.9 dB with L_1 increasing from 175 to 195 mm. The increment speed slows down when L_1 is beyond 190 mm.

The heights of the two PIFAs, i.e., h_1 and h_2, are identical with each other to ensure similar radiation performances for the two PIFAs to obtain equal amplitudes for the two orthogonal polarizations. The final height of the proposed antenna is optimized to 0.05 λ_0 for the compromise of the bandwidth and profile.

The energy of the feed probe will be equally allocated to two PIFAs only if the impedances of the two PIFAs are identical with each other. The impedance of a PIFA is dependent on the feed position along the resonant edge and independent of that along the nonresonant edge, thus that of the upper PIFA can be tuned with the feed position varied along the *y*-axis, while that of the lower PIFA can be tuned with the feed position varied along the *x*-axis. In order to acquire identical impedances for the two PIFAs, the feed position is tuned along the diagonal at first, i.e., $L_f = W_f$. After obtaining a rough position, then it is finely tuned around this diagonal position to acquire an optimized energy allocation.

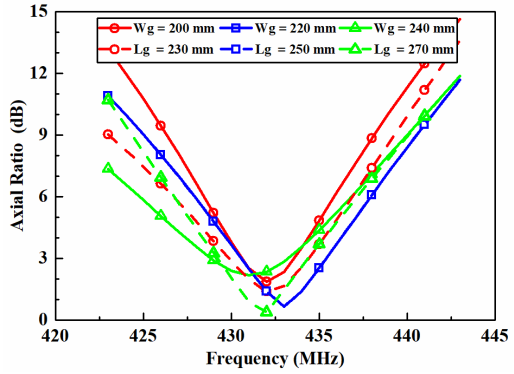

Fig. 6. Simulated AR against frequency for different W_g and L_g.

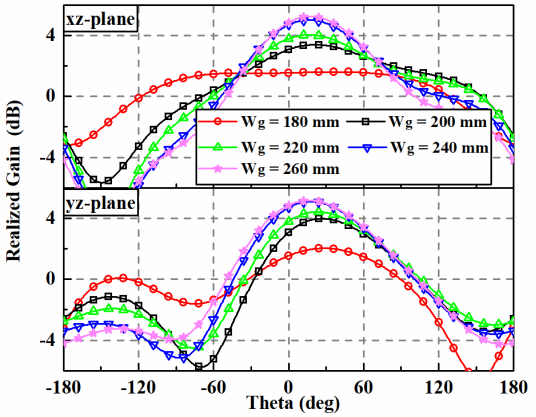

Fig. 7. Simulated radiation patterns in the *xz* and *yz* planes for different W_g.

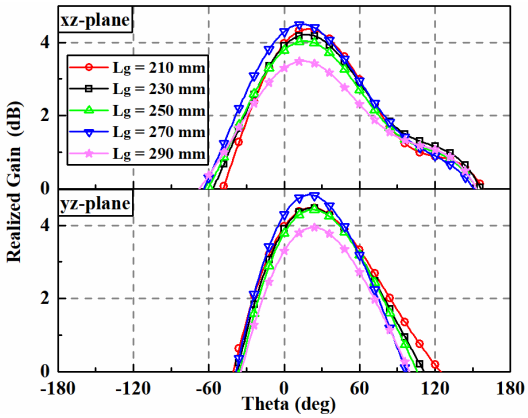

Fig. 8. Simulated radiation patterns in the *xz* and *yz* planes for different L_g.

The size of the ground plane is also of major significance for the proposed antenna. A compact ground plane with the size of 250 × 220 mm^2 is employed in this model for the application of the size-limited environment. The resonant frequency and bandwidth of the PIFAs will be slightly influenced by the size of the ground plane, thus the AR will be slightly affected by the variations of W_g and L_g as shown in Fig. 6. However, the gain will be impacted seriously by W_g because it is along the resonant edge of the lower PIFA. As plotted in Fig. 7, the maximum gain increases with the growing of W_g. If W_g reaches beyond 240 mm, the increment speed slows down. As for L_g, which is along the nonresonant edge of the lower PIFA, has little impact on the gain as shown in Fig. 8.

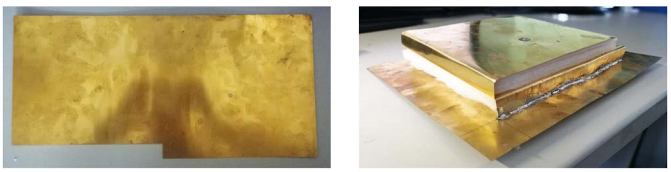

(a) (b)

Fig. 9. Photographs of the raw material and proposed antenna. (a) Brass plate before folding. (b) Proposed dual-layer PIFA.

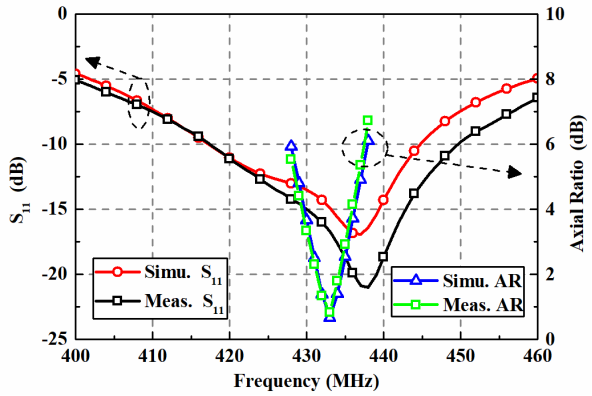

Fig. 10. Simulated and measured reflection coefficients and ARs of the proposed dual-layer PIFA.

III. Antenna Fabrication and Measurement Results

In order to validate the performance of the proposed dual-layer PIFA, a prototype was fabricated with two pieces of brass plates. Fig. 9(a) is a piece of irregular brass plate, which is employed to fold into the main body of the proposed dual-layer PIFA. It is cut by the laser cutting machine, the cutting error of which is less than 0.1 mm. The thickness of the brass plate is 0.2 mm, which is easy to fold by hand. Another piece of rectangular brass plate is employed to serve as the metal ground plane. The surface IV of the PIFA is soldered with the ground plane. To guarantee the stiffness of the antenna, the foam ($\varepsilon_r = 1.06$) is applied to sustain the antenna, and it has little impact on the antenna performance due to the low dielectric constant and loss. A 50 Ω SMA connector is soldered for the test, and the outer conductor of which is soldered on the back side of the ground plane, while the inner conductor of which is soldered with a probe to feed the dual-layer PIFA. The probe passes through the hole on the surface III and soldered on the surface I. The photograph of the final antenna is shown in Fig. 9(b).

A. S-Parameter

The simulated and measured reflection coefficients of the dual-layer PIFA are shown in Fig. 10, the simulated −10 dB impedance bandwidth is 6.4% (417–445 MHz), while the measured result is 7.2% (417–449 MHz).

B. AR and Radiation Performance

To estimate the AR and radiation performance of the proposed antenna, it is measured in a far-field anechoic chamber as shown in Fig. 11. The antenna under test is placed on a rotating platform, and a 433 MHz three-element Yagi–Uda antenna is utilized to act as the test probe. The distance between them is 4.5 m to satisfy the far-field condition. The broadside AR against frequency is shown in Fig. 10, the simulated and measured 3 dB AR bandwidths are

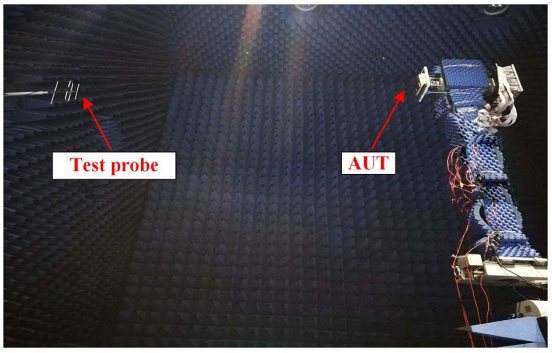

Fig. 11. Photograph of the radiation measurement setup.

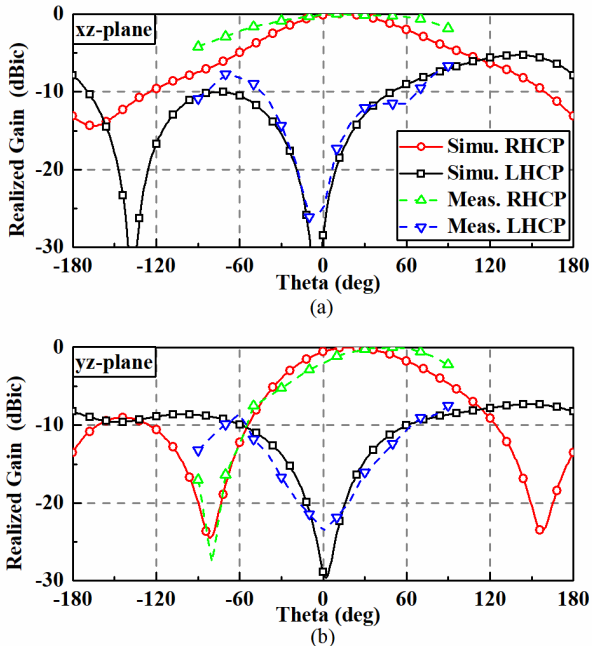

Fig. 12. Simulated and measured normalized CP radiation patterns at 433 MHz of the proposed dual-layer PIFA. (a) *xz* plane. (b) *yz* plane.

1.1% (430.6–435.4 MHz) and 1.1% (430.3–435.1 MHz), respectively. A good consistence is acquired between the simulated and measured results. The bandwidth is wide enough for the application of the active RFID systems.

The normalized simulated and measured RHCP and LHCP radiation patterns in the *xz* and *yz* planes are shown in Fig. 12. A good RHCP radiation is achieved around the broadside of the antenna. The maximum RHCP gain is 4.35 dBic, but it deviates to $\theta = 20°$ in the *yz* plane due to the asymmetric boundary of the PIFA. The broadside RHCP gain is 3.84 dBic with a gain drop of 0.51 dB, which meets the requirement of the active RFID reader.

Fig. 13 illustrates the simulated and measured AR beamwidth at 433 MHz. As shown in the figure, the 3 dB AR beamwidth is 45° (from −25° to 20°) in the *xz* plane and 44° (from −17° to 27°) in the *yz* plane. The AR beamwidth is deviated due to the asymmetric radiation pattern. The simulated and measured broadside RHCP gains are illustrated in Fig. 14, the gain fluctuation at the desired band (AR < 3 dB) is flat, but the maximum RHCP gain is slightly deviated to 437 MHz. The simulated total efficiency is also shown in Fig. 14, and the efficiency is higher than 97% across the desired band. The high efficiency is achieved due to the following two reasons:

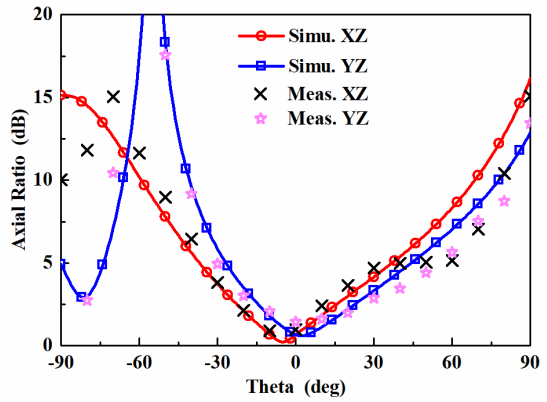

Fig. 13. Simulated and measured AR beamwidth at 433 MHz in the *xz* and *yz* planes.

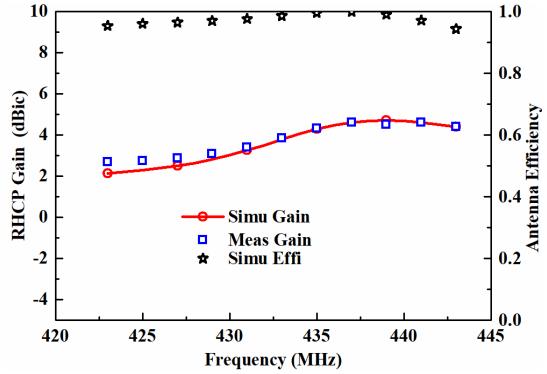

Fig. 14. Simulated and measured boresight realized gain and simulated efficiency of the proposed dual-layer PIFA.

TABLE II
COMPARISONS OF THE COMPACT SINGLE-FEED CP ANTENNAS

Ref.	Dimension (λ_0^3)	S_{11} BW	AR BW	Broadside Gain (dBic)	ε_r
[3]	0.30×0.30×0.03	>6.55%	3.28%	2.69	8
[4]	0.17×0.17×0.02	0.5%	0.6%	2.7	1
[8]	0.28×0.28×0.14	10.4%	2.92%	NG.	1
[20]	0.27×0.27×0.01	1.88%	0.67%	3.7	3.38
[21]	0.29×0.29×0.01	2.5%	0.5%	4	3.38
Proposed	0.26×0.22×0.05	7.2%	1.1%	3.8	1.06

1) low dielectric loss of the sustained foam and 2) low metal loss at such low frequency.

IV. DISCUSSION AND CONCLUSION

To highlight the merits of the proposed compact single-fed CP antenna, a comparison chart is illustrated in Table II. Lee *et al.* [3] proposed a compact ring microstrip antenna with high dielectric constant ($\varepsilon_r = 8$), but the gain and efficiency are affected because of the high dielectric loss. References [4] and [8] are an all-metal structure with air media and they both have the merits of low cost and ease of manufacture. Yu and Lim [4] proposed a more compact CP antenna, but the bandwidth is limited and the metal-mountable characteristic is not mentioned. Reference [8] is compact and has adequate bandwidth, but the profile is as high as 0.14 λ_0. Nasimuddin *et al.* [20], [21] proposed patch antennas with four asymmetric slots or slits to generate a CP radiation. They both have lower profile, but the bandwidth of them is narrow. As a consequence, the proposed dual-layer PIFA antenna is a novel structure with compact size and adequate bandwidth for the CP RFID reader.

This communication gives a feasible solution for the low-cost compact single-feed CP antenna. By stacking two orthogonal-placed $\lambda/4$ resonant PIFAs, a CP antenna with compact volume of 0.26 × 0.22 × 0.05 λ_0^3 is achieved, which has about 75% size reduction compared with the conventional corner-truncated patch antenna. The measured −10 dB impedance bandwidth and 3 dB AR bandwidth are 32 MHz (7.2%) and 4.8 MHz (1.1%), respectively. The broadside CP gain is 3.8 dBic and the simulated efficiency is higher than 97% across the 3 dB AR bandwidth. In a word, the proposed antenna has the merits of compact, low cost, lightweight, adequate bandwidth and gain, high efficiency, and ease of manufacture, thus it is suitable for the application of the active RFID reader.

REFERENCES

[1] S. Gao, Q. Luo, and F. Zhu, *Circularly Polarized Antennas*. Hoboken, NJ, USA: Wiley, 2014.

[2] K.-L. Wong, *Compact and Broadband Microstrip Antennas* (Compact Circularly Polarized Microstrip Antennas). Hoboken, NJ, USA: Wiley, 2002, ch. 5.

[3] D. Lee, P. Park, J. Kim, and J. Choi, "Aperture-coupled UHF RFID reader antenna for a handheld application," *Microw. Opt. Technol. Lett.*, vol. 50, no. 5, pp. 1261–1263, May 2008.

[4] J. J. Yu and S. Lim, "Design of an electrically small, circularly polarized, parasitic array antenna for an active 433.92-MHz RFID handheld reader," *IEEE Trans. Antennas Propag.*, vol. 60, no. 5, pp. 2549–2553, May 2012.

[5] S. Lim, J. Chen, and C. Cato, "Design of a thin, electrically small, two-element parasitic array with circular polarization," *IEEE Antennas Wireless Propag. Lett.*, vol. 17, no. 6, pp. 1006–1009, Jun. 2018.

[6] S. X. Ta, I. Park, and R. W. Ziolkowski, "Broadband electrically small circularly polarized directive antenna," *IEEE Access*, vol. 5, pp. 14657–14663, 2017.

[7] H. K. Ryu, S. Lim, and J. M. Woo, "Design of electrically small, folded monopole antenna using C-shaped meander for active 433.92 MHz RFID tag in metallic container application," *Electron. Lett.*, vol. 44, no. 25, pp. 1445–1447, Dec. 2008.

[8] X. Yang, Y. Z. Yin, W. Hu, and S. Li. Zuo, "Low-profile, small circularly polarized inverted-L antenna with double-folded arms," *IEEE Antennas Wireless Propag. Lett.*, vol. 9, pp. 767–770, 2010.

[9] L. Ukkonen, L. Sydänheimo, and M. Kivikoski, "Read range performance comparison of compact reader antennas for a handheld UHF RFID reader," in *Proc. IEEE Int. Conf. RFID*, May 2007, pp. 63–70.

[10] K. Finkenzeller, *RFID Handbook: Fundamentals and Applications in Contactless Smart Cards and Identification*, 2nd ed. Hoboken, NJ, USA: Wiley, 2004.

[11] *Information Technology—Radio Frequency Identification for Item Management—Part 7: Parameters for Active Air Interface Communications at 433 MHz*, standard ISO/IEC 18000-7, 2009.

[12] H. Iwasaki, "A circularly polarized small-size microstrip antenna with a cross slot," *IEEE Trans. Antennas Propag.*, vol. 44, no. 10, pp. 1399–1401, Oct. 1996.

[13] H.-M. Chen and K.-L. Wong, "On the circular polarization operation of annular-ring microstrip antennas," *IEEE Trans. Antennas Propag.*, vol. 47, no. 8, pp. 1289–1292, Aug. 1999.

[14] W.-S. Chen, C.-K. Wu, and K.-L. Wong, "Square-ring microstrip antenna with a cross strip for compact circular polarization operation," *IEEE Trans. Antennas Propag.*, vol. 47, no. 10, pp. 1566–1568, Oct. 1999.

[15] W.-S. Chen, C.-K. Wu, and K.-L. Wong, "Novel compact circularly polarized square microstrip antenna," *IEEE Trans. Antennas Propag.*, vol. 49, no. 3, pp. 340–342, Mar. 2001.

[16] F.-S. Chang, K.-L. Wong, and T.-W. Chiou, "Low-cost broadband circularly polarized patch antenna," *IEEE Trans. Antennas Propag.*, vol. 51, no. 10, pp. 3006–3009, Oct. 2003.

[17] K.-F. Tong and T.-P. Wong, "Circularly polarized U-slot antenna," *IEEE Trans. Antennas Propag.*, vol. 55, no. 8, pp. 2382–2385, Aug. 2007.

[18] C.-Y.-D. Sim and T.-Y. Han, "GPS antenna design with slotted ground plane," *Microw. Opt. Technol. Lett.*, vol. 50, no. 3, pp. 818–821, Mar. 2008.

[19] Nasimuddin, Z. N. Chen, and X. Qing, "Compact circularly polarized asymmetric-slotted microstrip patch antennas," *Microw. Opt. Technol. Lett.*, vol. 54, no. 8, pp. 1920–1927, Aug. 2012.

[20] Nasimuddin, Z. N. Chen, and X. Qing, "Asymmetric-circular shaped slotted microstrip antennas for circular polarization and RFID applications," *IEEE Trans. Antennas Propag.*, vol. 58, no. 12, pp. 3821–3828, Dec. 2010.

[21] Nasimuddin, X. Qing, and Z. N. Chen, "Compact asymmetric-slit microstrip antennas for circular polarization," *IEEE Trans. Antennas Propag.*, vol. 59, no. 1, pp. 285–288, Jan. 2011.

[22] H. Wong, K. K. So, K. B. Ng, K. M. Luk, C. H. Chan, and Q. Xue, "Virtually shorted patch antenna for circular polarization," *IEEE Antennas Wireless Propag. Lett.*, vol. 9, pp. 1213–1216, 2010.

[23] K. K. So, H. Wong, K. M. Luk, and C. H. Chan, "Miniaturized circularly polarized patch antenna with low back radiation for GPS Satellite Communications," *IEEE Trans. Antennas Propag.*, vol. 63, no. 12, pp. 5934–5938, Dec. 2015.

[24] P. C. Sharma and K. C. Gupta, "Analysis and optimized design of single feed circularly polarized microstrip antennas," *IEEE Trans. Antennas Propag.*, vol. AP-31, no. 6, pp. 949–955, Nov. 1983.

[25] J. R. James, P. S. Hall, and C. Wood, *Microstrip Antenna Theory and Design*. Stevenage, U.K.: Peregrinus, 1981.